Rare Metal Materials and Engineering
Volume 50, Issue 5, May 2021
Available online at www.rmme.ac.cn

Science Press

Cite this article as: Qi Dongli, Chen Jianjin, Liu Jun, et al. Influence of Molybdenum Addition on Oxidation Resistance of CrN Coatings[J].Rare Metal Materials and Engineering,2021,50(05):1505-1512.

ARTICLE

Influence of Molybdenum Addition on Oxidation Resistance of CrN Coatings

Qi Dongli, Chen Jianjin, Liu Jun, Lv Wei, Song Jianyu, Shen Longhai

School of Science, Shenyang Ligong University, Shenyang 110159, China

Abstract: To investigate the effect of molybdenum (Mo) addition on microstructure and oxidation resistance of CrN coating, Cr-Mo-N coatings with different Mo contents were fabricated on silicon wafers and high speed steel by reactive magnetron sputtering and annealed at elevated temperatures from 500 °C to 800 °C in air for 1 h. The coatings before and after annealing were characterized by X-ray diffraction (XRD), Raman spectroscopy and scanning electron microscope (SEM). The results show that the as-deposited CrN and Cr-Mo-N coatings all exhibit B1 face-centered cubic (fcc) phase based on the CrN lattice. Mo ions substitute for Cr ions in Cr-N lattice, forming the solid solution Cr-Mo-N coatings. At 600 °C, XRD and Raman spectra show that the MoO_3 phase forms in Cr-Mo-N coatings with higher Mo contents, indicating a coarser surface with higher oxygen content. At 700 °C, the cross sectional morphology of the CrN coating exhibits loose columnar grains with some porous regions due to the internal stress while the Cr-Mo-N coating shows the dense columnar structure. This study reveals that the Cr-Mo-N coatings with lower Mo contents (<17at%) have better oxidation resistance than the CrN coating does.

Key words: Cr-Mo-N coating; magnetron sputtering; Raman; oxidation resistance

Transition metal nitride coatings are widely used in cutting tools in order to reduce the tool cost and extend the tool life for past decades[1-3]. It is generally known that the coated tools not only exhibit extreme mechanical properties, but also withstand potentially aggressive operating environments. For example, the temperature at cutting edge can reach as high as 700~900 °C during dry or high speed machining[4-6]. Recently, the interest of green manufacturing has promoted the development of coatings for dry machining[7-9]. As the friction coefficient of coating in the cutting process decreases, the friction heat, as the kinetic energy for high temperatures, decreases, and then the use of lubricant reduces along with power requirements[10]. Therefore, the coatings with lower friction coefficient is a developing direction of green manufacturing techniques.

CrN coating is a promising hard coating material due to its high hardness, excellent wear and oxidation resistance at about 700 °C[11-13]. The friction properties of metal nitride coatings improve by incorporating elements which form the high temperature lubricious oxides[14-17]. Such lubricious oxides, often referred as “Magnéli phase”, form by friction and/or thermal oxidation of Mo_2N coatings[18,19]. Accordingly, ternary Cr-Mo-N coatings can have superior properties through optimal combinations of CrN and Mo-N[20-23]. The hardness value of the Cr-Mo-N coatings after doping 21at% molybdenum by hybrid arc ion plating-direct current (AIP-DC) sputtering increases from 18 GPa (pure CrN) to about 34 GPa, and the corresponding friction coefficient decreases from 0.49 for pure CrN to 0.37 for Cr-Mo-N coating with 30.4at% molybdenum[22]. However, little information presents the oxidation resistance of the Cr-Mo-N coatings.

The purposes of this research are to synthesize Cr-Mo-N coatings and show the influence of molybdenum addition on the structure and oxidation resistance of CrN films at high temperature.

1 Experiment

Cr-Mo-N coatings were deposited on the polished high speed steel (HSS) substrates and silicon wafers by reactive magnetron sputtering in a mixture atmosphere of argon and ni-

---

Received date: May 29, 2020
Foundation item: Natural Science Foundation Guidance Plan Project of Liaoning (2019-ZD-0254)
Corresponding author: Shen Longhai, Ph. D., Professor, School of Science, Shenyang Ligong University, Shenyang 110159, P. R. China, Tel: 0086-24-24682189, E-mail: 27869613@qq.com

trogen with the purity of 99.999% for both gases. Details of the deposition apparatus were presented in the previous work[24]. The HSS substrates were ground and polished by diamond paste of 1 μm in size, and then ultrasonically cleaned in acetone for 15 min and ethanol for 15 min before deposition. Pure Cr (diameter of 60 mm, thickness of 5 mm, purity of 99.9%) and Mo (diameter of 60 mm, thickness of 5 mm, purity of 99.9%) were attached to the sputter sources. Both the targets were pre-sputtered for 15 min to remove the surface oxides and contaminants after the base pressure of the chamber was less than 5×10^{-4} Pa. During the coating deposition, the total working pressure was maintained at 0.50 Pa and the Ar and N_2 flow rates were sustained at 30 cm^3/min. The substrate temperature was kept at 200 °C. Mo content of the Cr-Mo-N coatings was controlled by varying two target currents. Firstly, the target current of Cr was kept at 0.4 A, and the target current of Mo was adjusted at 0, 0.2, 0.3 and 0.4 A, separately. The samples under each condition were marked as CrN, Cr-Mo-N-1, Cr-Mo-N-2, Cr-Mo-N-3 respectively. Then, the target current of Mo was kept at 0.4 A, and the target current of Cr was adjusted at 0.3 and 0.2 A, separately. The samples under each condition were marked as Cr-Mo-N-4 and Cr-Mo-N-5, respectively. The oxidation was carried out in air between 500 and 800 °C for 1 h with a heating rate of 10 °C/min. After the increase of oxidation time, the furnace was cooled to ambient temperature slowly.

Crystal structure of the Cr-Mo-N coatings before and after oxidation was characterized by X-ray diffraction (XRD, D/MAX-RA of Rigaku, Japan) with monochromatic Cu Kα (λ=0.154 056 nm). Table 1 shows the composition of different samples and their grain size calculated from the width of XRD peaks by Debye-Scherrer equation. Scanning electron microscope (SEM, S-3400N, Hitachi, Japan) was used to observe the surface and cross-sectional morphologies and obtain structure and thickness information of the coatings. Energy dispersive spectroscope (EDS) coupled with the SEM was used to analyze the chemical composition of coatings. The formed oxides were investigated by Raman spectroscopy using a Jobin-Yvon Raman spectrometer. The excitation source was a 532 nm laser (50 mW power).

Table 1 Chemical composition, grain size and deposition rate of Cr-Mo-N coatings

Sample	Chemical composition/at%			Grain size/nm	Deposition rate/$nm\cdot s^{-1}$
	Cr	Mo	N		
CrN	51.03	0	48.97	13.8	0.35
Cr-Mo-N-1	35.75	9.63	54.62	16.6	0.23
Cr-Mo-N-2	30.20	13.58	56.22	14.4	0.25
Cr-Mo-N-3	27.86	17.36	54.78	13.6	0.27
Cr-Mo-N-4	24.17	21.13	54.70	17.2	0.22
Cr-Mo-N-5	22.03	23.67	54.30	22.7	0.20

2 Results and Discussion

2.1 Influence of molybdenum addition on the structure of CrN coatings

The chemical composition of Cr-Mo-N coatings (measured by EDS) is listed in Table 1. As expected, Mo content increases from 0at% to 23.67at% with the change of two target currents, while Cr content shows a decreasing trend from 51.03at% to 22.03at%. Fig.1 shows the XRD patterns of CrN and Cr-Mo-N coatings with different Mo contents. Apart from body-centered cubic Cr phase, the as-deposited coatings exhibit B1 face-centered cubic (fcc) phase based on the CrN lattice. The four diffraction peaks correspond to the (111), (200), (220) and (311) planes of fcc structure with a clearly preferential growth along (200). Oh et al[25] pointed out that the preferred orientation of (200) appears as the surface energy dominates and the preferred orientation of (111) appears as the strain energy dominates. Therefore, the conclusion is that the surface energy plays an important role during the deposition of Cr-Mo-N coatings. It can be seen that the lower the deposition rate, the better the crystallinity (Table 1). High deposition rate stops grain growth and stimulates the renucleation of

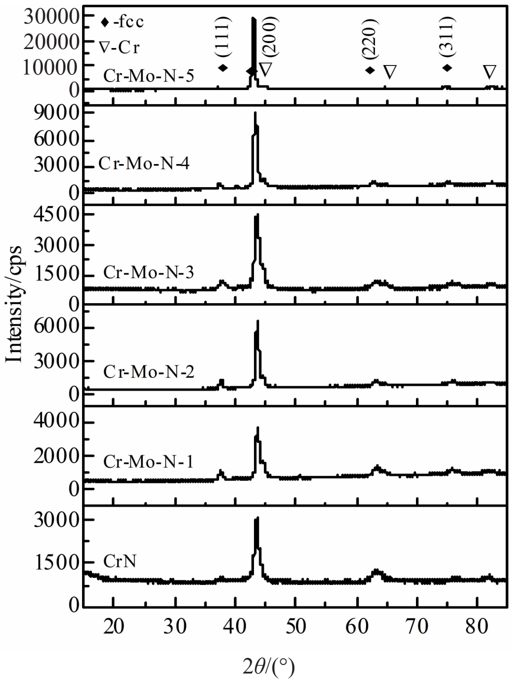

Fig.1 XRD patterns of as-deposited CrN and Cr-Mo-N coatings with different Mo contents

grains, resulting in the smaller grain size[26]. Furthermore, with increasing the Mo content, the diffraction peaks also shift to lower diffraction angles, thereby implying an increase in lattice parameters, which is a sign of the formation of solid solution CrMoN and the substitution of Cr atoms by Mo atoms. This structure evolution of the coatings is similar to the results about Cr-Mo-N and Mo-W-N coatings[20,27].

The SEM images of the cross-sectional morphologies of Cr-Mo-N coatings with different Mo contents are shown in Fig.2. The Cr-Mo-N-1, Cr-Mo-N-4 and Cr-Mo-N-5 coatings with the lower deposition rate show a typical columnar structure. The CrN, Cr-Mo-N-2 and Cr-Mo-N-3 coatings with a higher deposition rate exhibit a fine-grained and dense morphology. More sputtered atoms reach the surface of the substrate per unit time due to the higher deposition rate. Accordingly, more heterogeneous nucleation sites are offered, which results in the grain refinement.

2.2 Influence of molybdenum addition on oxidation resistance of CrN coatings at high temperature

Fig.3 illustrates the XRD patterns of the Cr-Mo-N coatings with different Mo contents after annealing at 600 °C in air for 1 h. The JCPDS cards used in this study are 85-1336 (Cr), 76-2494 (CrN), 38-1479 (Cr_2O_3) and 35-0609 (MoO_3). It can be seen that the diffraction peaks of fcc structure are well maintained in the Cr-Mo-N coatings with different Mo contents (Fig. 3a). Besides, the weak (012) and (104) peaks of Cr_2O_3 can be identified in the CrN coating and the weak MoO_3 peaks can be detected in the Cr-Mo-N-5 coating (Fig.3b). The reason for the appearance of MoO_3 phase is that a small amount of Mo_2N phases form in the Cr-Mo-N coatings with higher Mo contents, which are easily oxidized. The diffraction peaks of molybdenum or chromium oxides cannot be found in XRD patterns of other Cr-Mo-N coatings with lower molybdenum contents, indicating that their oxidation resistance is better than that of CrN and Cr-Mo-N coatings with higher molybdenum contents at 600 °C.

The structure of oxides is often analyzed by Raman spectroscopy. Fig.4 presents Raman spectra of the Cr-Mo-N coatings after annealing at 600 °C in air for 1 h. The Raman spectra of the Cr-Mo-N-4 and Cr-Mo-N-5 coatings exhibit typical peaks centered at 905 and 773 cm^{-1}, respectively, corresponding to the β-MoO_3[28]. The Raman spectrum of CrN coating shows a peak of Cr_2O_3 at 554 cm^{-1}[29]. The oxides cannot be identified through Raman spectra for Cr-Mo-N-1, Cr-Mo-N-2 and Cr-Mo-N-3 coatings, implying that these coatings have better oxidation resistance.

Oxygen content of the Cr-Mo-N coatings with different Mo contents (measured by EDS) is shown in Fig. 5. The oxygen content of Cr-Mo-N coatings with lower Mo contents is around 10at%. The oxygen content of the Cr-Mo-N coatings increases sharply with increasing the Mo contents. These results show that the addition of low Mo contents improves the oxidation resistance of the CrN coatings, while the high Mo contents obviously weakens the coating oxidation resistance.

Fig. 6 displays the surface morphologies of the Cr-Mo-N coatings with different Mo contents after annealing at 600 °C in air for 1 h. The Cr-Mo-N-1, Cr-Mo-N-2 and Cr-Mo-N-3 coatings exhibit a smoother fine-grained morphology. The oxide particles with granular and faceted structure on the top of the oxidized CrN coating were observed. The Cr-Mo-N-4 and Cr-Mo-N-5 coatings show a rougher surface of oxide scale with bigger grains and cavities or pores. The generation and release of N_2 during oxidation result in the formation of cavi-

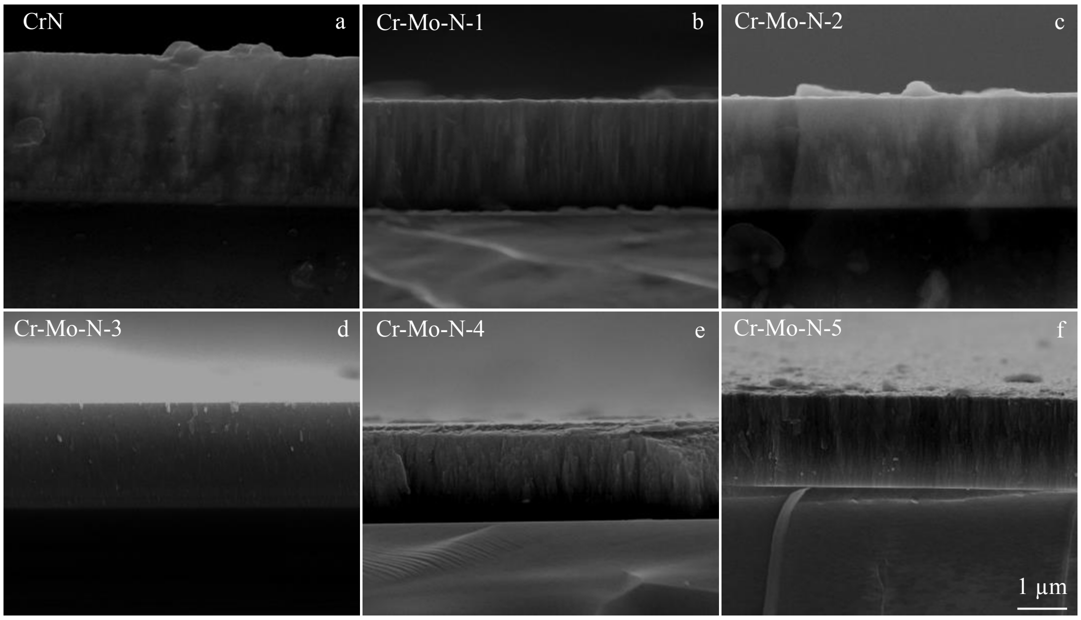

Fig.2 Cross-sectional morphologies of Cr-Mo-N coatings with different Mo contents: (a) CrN, (b) Cr-Mo-N-1, (c) Cr-Mo-N-2, (d) Cr-Mo-N-3, (e) Cr-Mo-N-4, and (f) Cr-Mo-N-5

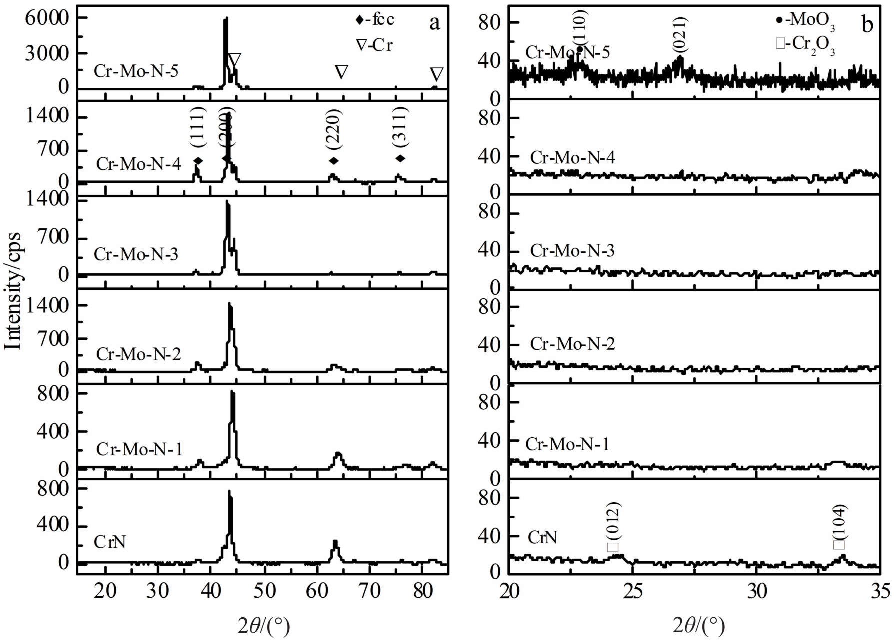

Fig.3 XRD patterns of Cr-Mo-N coatings with different Mo contents after annealing at 600 °C in air for 1 h: (a) 2θ: 20°~80° and (b) 2θ: 20°~35°

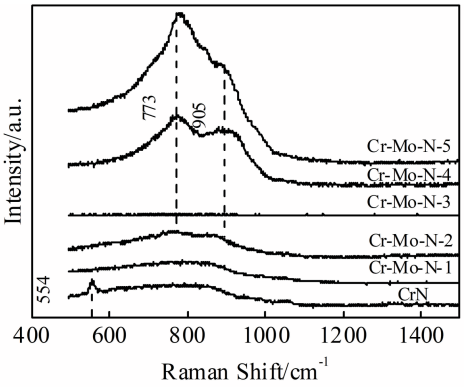

Fig.4 Raman spectra of Cr-Mo-N coatings with different Mo contents after annealing at 600 °C in air for 1 h

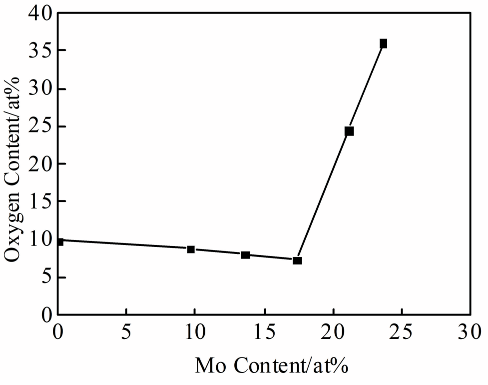

Fig.5 Oxygen content of Cr-Mo-N coatings with different Mo contents after annealing at 600 °C in air for 1 h

ties or pores[30].

2.3 Oxidation resistance of CrN and Cr-Mo-N-3 coatings at elevated temperatures

The XRD patterns of the CrN coatings before and after annealing from 500 °C to 800 °C are presented in Fig.7. C-CrN (111), (200) and (220) peaks are thermally stable at 600 °C. The diffraction peaks of the as-deposited CrN coating located at 36.81°, 43.11° and 62.53° are CrN (111), CrN (200) and CrN (220), respectively, which shift toward lower angles according to JCPDF No.76-2494. The reason for the peak shift is the residual compressive stress in the as-deposited CrN coating. The diffraction peaks shift to higher angles with the increase of annealing temperature, which implies the stress relaxation for the CrN coating during heat treatment[31]. When the samples are heated at 700 °C, XRD analysis of CrN coatings shows the CrN phase with a very small fractions of Cr_2O_3. After heat treatment at 800 °C for 1 h, only the matrix peaks are detected, suggesting that the coating basically exfoliates.

For Cr-Mo-N-3 coating, fcc phases are well maintained at 700 °C, as shown in Fig.8. With the increase of annealing temperature, the (111) peak intensity increases while the (200) peak intensity decreases and the diffraction peaks shift to higher angles. The variation of the diffraction peak is attributed to the stress relaxation. At 800 °C, (012), (104) and (024) peaks of Cr_2O_3 appear in the Cr-Mo-N-3 coating.

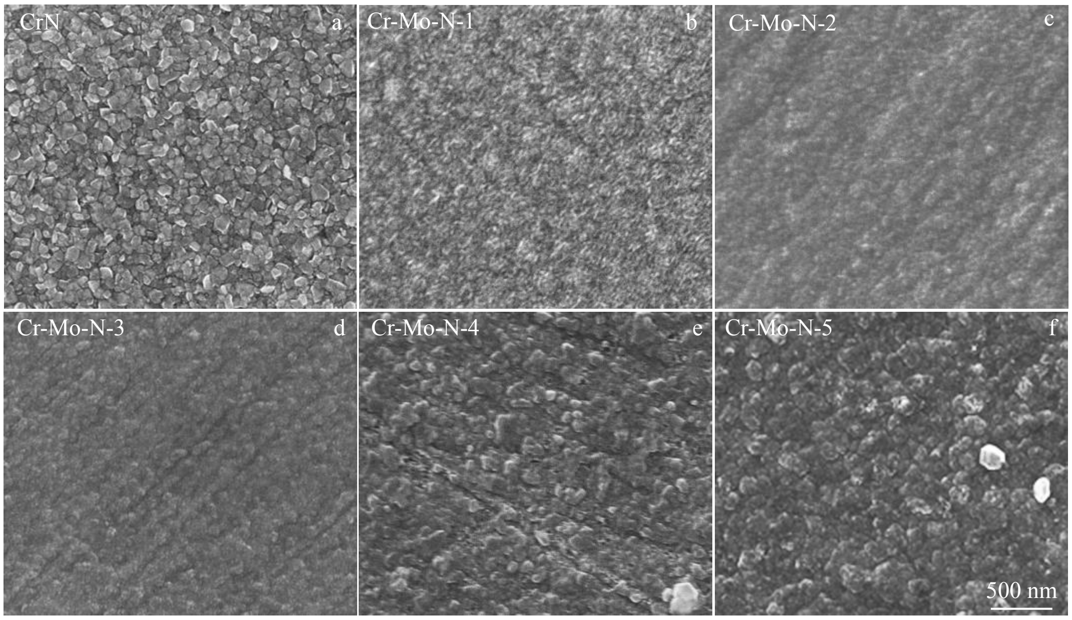

Fig.6 SEM images of surface morphology of Cr-Mo-N coatings on HSS with different Mo contents after annealing at 600 °C in air for 1 h: (a) CrN, (b) Cr-Mo-N-1, (c) Cr-Mo-N-2, (d) Cr-Mo-N-3, (e) Cr-Mo-N-4, and (f) Cr-Mo-N-5

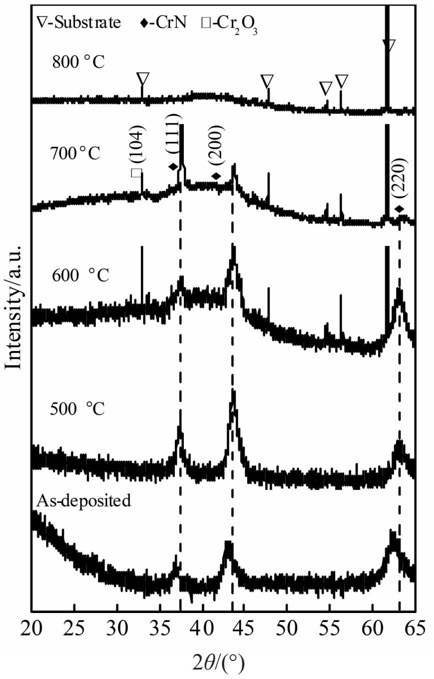

Fig.7 XRD spectra of CrN coatings on Si substrates before and after annealing in air at different temperatures for 1 h

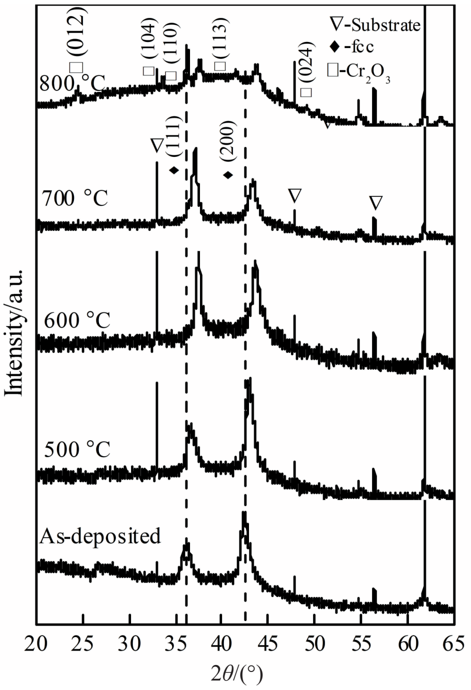

Fig.8 XRD spectra of Cr-Mo-N-3 coatings on Si substrates before and after annealing in air at different temperatures for 1 h

The Mo-oxides are not observed in the XRD patterns at test temperatures for the following reasons: (1) Cr_2O_3-based oxide containing molybdenum forms; (2) even if a small amount of Mo-oxides form, the volatilization reaction rate is higher than the oxidation reaction rate above 550 °C[32].

Table 2 lists the chemical composition of as-deposited and air-annealed CrN and Cr-Mo-N-3 coatings on Si substrates. With increasing the annealing temperature to 700 °C, the oxygen content of CrN and Cr-Mo-N-3 coatings increases to 28.35at% and 24.45at%, respectively. Only a small amount of

Table 2 Chemical composition of as-deposited and annealed CrN and Cr-Mo-N-3 coatings on Si substrates

Sample	Temperature/°C	Element content/at%				Mo/Cr
		N	O	Cr	Mo	
CrN	As-deposited	51.23	0	48.77	-	-
	500	44.56	11.97	43.47	-	-
	600	42.39	15.45	42.16	-	-
	700	38.45	28.35	33.20	-	-
	800	-	7.05	6.62	-	-
Cr-Mo-N-3	As-deposited	55.21	0	26.47	18.32	0.69
	500	51.71	7.30	24.45	16.54	0.67
	600	48.52	13.50	23.62	14.36	0.61
	700	41.33	24.45	22.82	11.40	0.50
	800	17.94	55.26	19.56	7.24	0.37

chromium and oxygen is detected in the CrN coating after annealing at 800 °C and most of the rest is the matrix component, suggesting that the coating basically exfoliates. The oxygen content of Cr-Mo-N-3 coating annealed at 800 °C is 55.26at% and the nitrogen content is 17.94at%, indicating that the some coatings are oxidized, and some initial coatings remain. The atomic ratio of Mo/Cr in Cr-Mo-N-3 coating decreases from 0.69 to 0.37, which means that a small amount of volatile molybdenum oxides form and more molybdenum oxides volatilize with the increase of annealing temperature[19,32].

The SEM images of surface and cross-section morphologies of CrN coatings on Si substrates before and after annealing in air at different temperatures for 1 h are demonstrated in Fig.9. The microstructure of CrN coating annealed at 700 and 800 °C in air for 1 h exhibits an appreciable change compared with the microstructure of as-deposited coating. After annealing at 700 °C in air for 1 h, the surface morphology displays the granular and faceted structure and the cross sectional morphology exhibits loose columnar grains with some porous regions in the Cr interlayer. The formation of the porous oxide regions is attributed to the formation of a large number of internal cracks due to the internal stress, which is caused by the difference of the thermal expansion coefficient between the substrates and coatings during the annealing process[33,34]. At 800 °C, the coat-

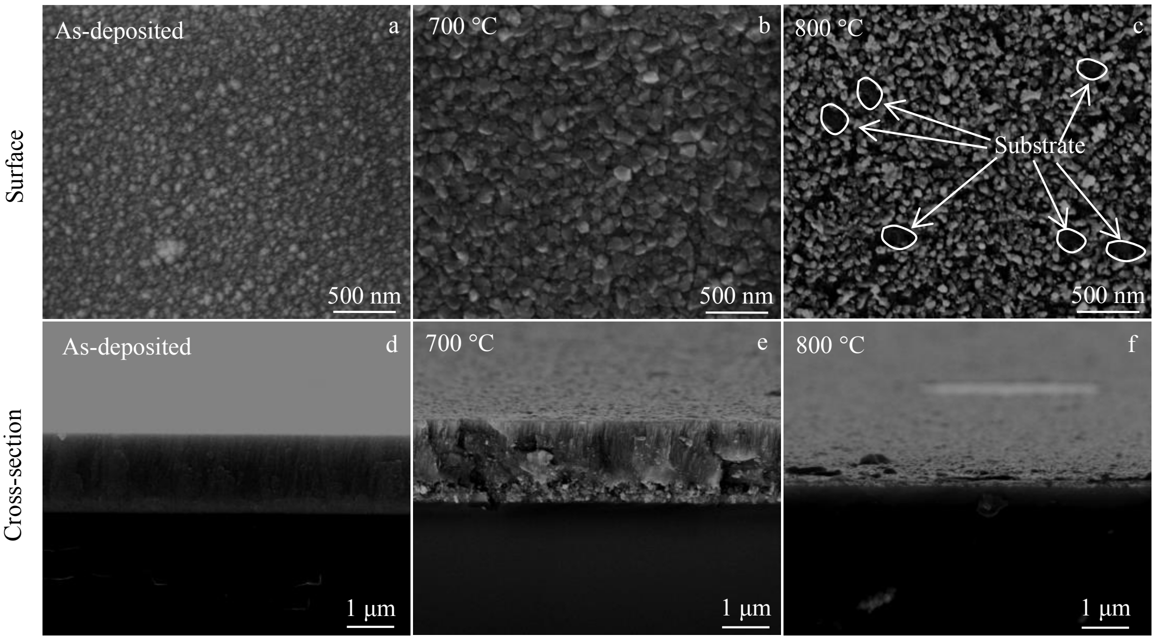

Fig.9 SEM images of surface (a~c) and cross-section (d~f) morphologies of CrN coatings on Si substrates before and after annealing in air at different temperatures for 1 h：(a, d) as-deposited，(b, e) 700 °C，and (c, f) 800 °C

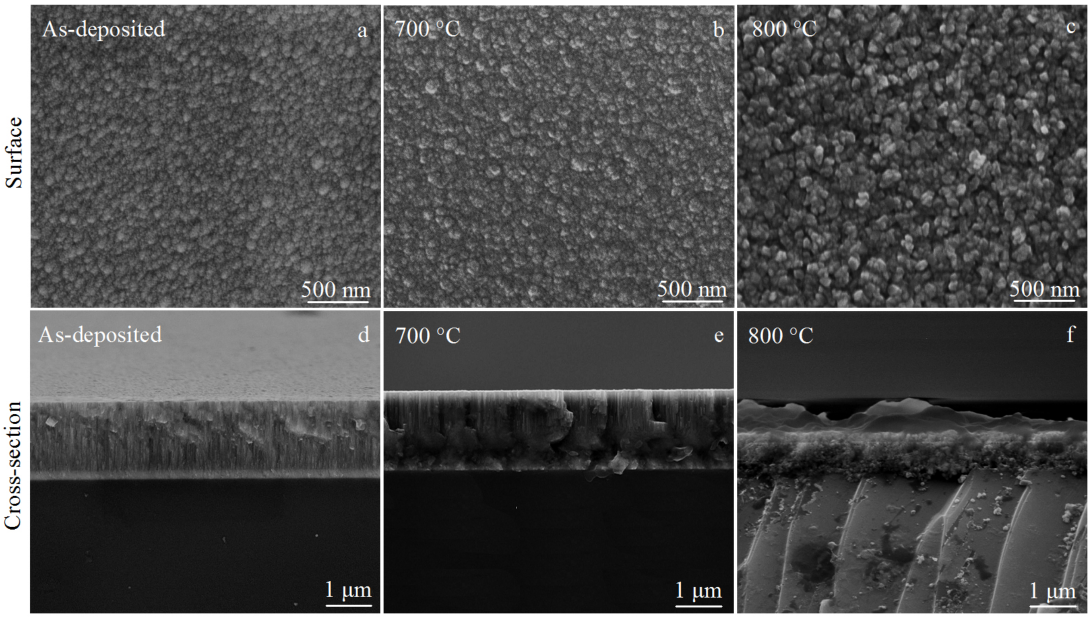

Fig.10 SEM images of surface (a~c) and cross-section (d~f) morphologies of Cr-Mo-N-3 coatings on Si substrates before and after annealing in air at different temperatures for 1 h: (a, d) as-deposited, (b, e) 700 °C, and (c, f) 800 °C

ing completely fails. There are few oxide particles on the surface of the matrix, and many areas are exposed. Nevertheless, for the Cr-Mo-N-3 coating annealed at 700 °C in air for 1 h, the surface morphology still shows a fine-grained and dense structure compared with that of the as-deposited coating (Fig. 10). The cross-sectional morphology reveals a dense columnar structure. The surface of the Cr-Mo-N-3 coating annealed at 800 °C becomes rough and porous and the columnar structure disappears. The above results indicate that the Cr-Mo-N-3 coating shows a better oxidation resistance than the CrN coating does on Si substrates.

3 Conclusions

1) The as-deposited CrN and Cr-Mo-N coatings all show a single phase fcc structure with a preferential growth along (200). The coatings with the lower deposition rate show a typical columnar structure.

2) After annealing at 600 °C in air for 1 h, the XRD and Raman results illustrate that Cr_2O_3 and MoO_3 phases appear in CrN and CrMoN coatings with high Mo content. The CrMoN coatings with relatively low Mo contents exhibit a smoother fine-grained morphology. The CrMoN coatings with relatively high Mo contents show a coarser surface with higher oxygen content.

3) After annealing at 700 °C in air for 1 h, the cross sectional morphology of the CrN coating exhibits loose columnar grains with some porous regions due to the internal stress, while the CrMoN coating shows dense columnar structure. After annealing at 800 °C in air for 1 h, the CrN coating basically exfoliates while some of the initial CrMoN coating remains.

4) The CrMoN coatings with lower molybdenum contents (<17at%) show better oxidation resistance than the CrN coating does. However, over doping of Mo has a detrimental effect on oxidation resistance of the coatings.

References

1 Jin Jie. *Rare Metal Materials and Engineering*[J], 2016, 45(12): 3325 (in Chinese)

2 Zhang Ting, Li Shuangming, Li Kewei *et al*. *Rare Metal Materials and Engineering*[J], 2015, 44(3): 697 (in Chinese)

3 Wang Yanfeng, Li Zhengxian, Wang Haonan *et al*. *Rare Metal Materials and Engineering*[J], 2017, 46(5): 1219

4 Khamseh S, Araghi H. *Ceramics International*[J], 2016, 42(8): 9988

5 Abukhshim N A, Mativenga P T, Sheikh M A. *International Journal of Machine Tools and Manufacture*[J], 2006, 46(7-8): 782

6 Karaguzel U, Budak E. *Journal of Materials Processing Technology*[J], 2018, 262: 532

7 Norrby N, Johansson-Jõesaar M P, Odén M. *Surface & Coatings Technology*[J], 2014, 257: 102

8 Hörling A, Hultman L, Odén M *et al*. *Surface & Coatings Technology*[J], 2005, 191(2-6): 384

9 Quesada F, Mariño A, Restrepo E. *Surface & Coatings Technology*[J], 2006, 201(6): 2925

10 Koshy R A, Graham M E, Marks L D. *Surface & Coatings Technology*[J], 2007, 202(4-7): 1123

11 Qi Z B, Liu B, Wu Z T *et al*. *Thin Solid Films*[J], 2013, 544: 515

12 Mayrhofer P H, Willmann H, Mitterer C. *Surface & Coatings Technology*[J], 2001, 146-147: 222

13 Lin J L, Zhang N Y, Sproul W D *et al. Surface & Coatings Technology*[J], 2012, 206(14): 3283

14 Aouadi S M, Gao H, Martini A *et al. Surface & Coatings Technology*[J], 2014, 257: 266

15 Qiu Y X, Zhang S, Lee J W *et al. Journal of Alloys and Compounds*[J], 2015, 618: 132

16 Stone D S, Harbin S, Mohseni H *et al. Surface & Coatings Technology*[J], 2013, 217: 140

17 Zeng Qunfeng, Chen Tong. *Journal of Non-Crystalline Solids* [J], 2018, 493: 73

18 Ürgen M, Eryilmaz O L, Çakir A F *et al. Surface & Coatings Technology*[J], 1997, 94-95: 501

19 Wang Tao, Zhang Guojun, Liu Zhuanning *et al. Ceramics International*[J], 2015, 41(5): 7028

20 Kim K H, Choi E Y, Hong S G *et al. Surface & Coatings Technology*[J], 2006, 201(7): 4068

21 Yoon C S, Kim K H, Kwon S H *et al. Journal of the Korean Physical Society*[J], 2009, 54(3): 1237

22 Xu Runxiang, Shi Wen, Chen Zhiyong. *Shanghai Metals*[J], 2009, 31(3): 20 (in Chinese)

23 Koshy R A, Graham M E, Marks L D. *Surf Coat Technol*[J], 2010, 204(9-10): 1359

24 Qi Dongli, Lei Hao, Fan Di *et al. Acta Metallurgica Sinica*[J], 2015, 51(3): 371 (in Chinese)

25 Oh U C, Je J H. *Journal of Applied Physics*[J], 1993, 74(3): 1692

26 Wu Z T, Qi Z B, Zhang D F *et al. Surface and Coatings Technology*[J], 2016, 289: 45

27 Yang J F, Yuan Z G, Zhang G G *et al. Materials Research Bulletin*[J], 2009, 44(10): 1948

28 Pham T T P, Nguyen P H D, Vo T T *et al. Materials Chemistry and Physics*[J], 2016, 184: 5

29 Khamlich S, Nuru Z Y, Bello A *et al. Journal of Alloys and Compounds*[J], 2015, 637: 219

30 Chen Y I, Lin Y T, Chang L C *et al. Surface and Coatings Technology*[J], 2011, 206(7): 1640

31 Barshilia H C, Rajam K S. *Surface and Coatings Technology* [J], 2004, 183(2-3): 174

32 Solak N, Ustel F, Urgen M *et al. Surface and Coatings Technology*[J], 2003, 174-175: 713

33 Liu Yanming, Li Tong, Liu Feng *et al. Acta Metallurgica Sinica (English Letters)*[J], 2019, 32(1): 136

34 Lin J, Moore J J, Wang J *et al. Thin Solid Films*[J], 2011, 519(8): 2402

钼添加对CrN涂层抗氧化性能的影响

齐东丽，陈建金，刘　俊，吕　伟，宋健宇，沈龙海

(沈阳理工大学 理学院，辽宁 沈阳 110159)

摘　要：研究钼添加对CrN涂层微观结构和抗氧化性能的影响，采用反应磁控溅射法在硅片和高速钢片上制备不同Mo含量的Cr-Mo-N涂层，并在500~800 ℃的高温空气中退火1 h，用X射线衍射（XRD）、拉曼光谱和扫描电子显微镜（SEM）对涂层退火前后的微观形貌进行表征。沉积的CrN和Cr-Mo-N涂层均表现出基于CrN晶格的B1面心立方相（fcc）。Mo离子取代Cr-N晶格中的Cr离子，形成Cr-Mo-N固溶体。在600 ℃时，XRD和拉曼光谱表明，Mo含量较高的Cr-Mo-N涂层中形成MoO_3相，表面较粗糙，含氧量较高。在700 ℃时，CrN涂层由于内应力的作用，其横截面形貌为疏松的柱状晶，并有一定的多孔区，而Cr-Mo-N涂层则为致密的柱状晶结构。低Mo含量（<17at%）的Cr-Mo-N涂层比CrN涂层具有更好的抗氧化性。

关键词：Cr-Mo-N涂层；磁控溅射；拉曼；抗氧化

作者简介：齐东丽，男，1978年生，博士，沈阳理工大学理学院，辽宁 沈阳 110159，电话：024-24682189，E-mail：285385997@qq.com